

Cross-species analysis of serum albumin: towards understanding function based on evolutionarily unique amino acids

Mary Grace I. Galinato*, Sean Artello, Emily M. Luteran, Alexandra Alfonso Castro and Michael Campbell

School of Science, Penn State Behrend, Erie, PA, USA.

ABSTRACT

Serum albumin (SA) is the most abundant protein in the circulatory system that functions as a repository for a host of molecules, including heme *b* (iron protoporphyrin IX). The crystal structure of the complex derived from humans, HSA-heme, shows heme binding in subdomain IB with several amino acids stabilizing the co-factor within the protein matrix. The residues are Tyr138, Tyr161, Ile142, His146, and Lys190. The complex itself resembles the active site of other heme enzymes such as catalase and globins (e.g. hemoglobin, Hb and myoglobin, Mb), which scavenge reactive nitrogen species (RNS) or transport oxygen, respectively. One of the goals of this work is to elucidate whether evolution retained these key amino acids, or if it added new variance to accommodate species-specific problems. Several of the species investigated in this work have various behavioral tendencies such as diving, migration, and hibernation, and we seek to determine the role of SA in heme binding and oxidative stress response in light of current literature. Cross-species analyses were carried out using Clustal Omega multiple sequence alignment of the key residues, while the potential for oxidative stress response *via* RNS reactions is investigated using absorption spectroscopy. Results demonstrate that the region of heme binding is fairly conserved throughout the species studied, at least in the properties of the amino acids, implying retention of function for heme coordination within the

subdomain. Absorption spectroscopy establishes RNS (e.g. nitric oxide) binding to HSA-heme, alluding to the complex's influence on oxidative stress correction.

KEYWORDS: (human) serum albumin, heme, amino acids, oxidative stress, reactive oxygen/nitrogen species, nitric oxide, nitrite, nitrite reductase, absorption spectroscopy, alignment.

INTRODUCTION

Human serum albumin (HSA) is one of the most prevalent proteins in plasma, and has multiple domains which are used for a range of functions and binding interactions. These domains give HSA an affinity for a wide variety of naturally-occurring and foreign compounds such as fatty acids, hormones, metal ions, co-factors (e.g. iron heme *b*), drugs and pharmaceuticals [1-10]. This remarkable affinity is used in a host of intrinsic bodily processes, and has linked HSA to pharmacokinetics and medical applications [11-14]. Given that HSA is the major protein in the circulatory system, the formation of a complex between HSA and heme has medical importance as it provides the framework for developing HSA-based blood substitutes. For example, a prior mutagenesis study generated recombinant HSA followed by heme *b* incorporation that activates the complex and show close O₂ binding affinities to those exhibited by myoglobin (Mb) and the high-affinity form of hemoglobin (Hb) [15]. The versatility of HSA allows it to achieve pseudo-enzymatic properties and the potential for induced functions of the protein, including binding of diatomic molecules

*Corresponding author: galinato@psu.edu

to the iron heme *b* center when this co-factor is incorporated [15-22]. One more useful property of HSA in the body is its role as an antioxidant due to its ligand-binding capabilities and ability to trap reactive oxygen (ROS) and nitrogen (RNS) species [23, 24].

During periods of acute hemolysis and heme overload, HSA may act as a heme reservoir with an affinity of $\sim 1/15^{\text{th}}$ that of Hb [25]. The ability of HSA to coordinate with iron heme *b* (vide infra) and form a heme enzyme complex [26] (referred to as HSA-heme) have implications on diatomic molecule binding and oxidative stress response. In itself, native HSA is inactive as a diatomic molecule binding protein but is activated in the presence of heme, behaving almost similar to Hb and Mb under the right conditions. Heme enzymes react with ROS (e.g. superoxide, O_2^- and peroxide, O_2^{2-}) and RNS (e.g. nitric oxide, NO, and peroxynitrite, ONOO^-) to scavenge and detoxify these species. For example, Hb, Mb, and flavoHbs detoxify NO in blood through nitric oxide dioxygenation (NOD), in which oxy-Hb/Mb/flavoHb (having partial superoxide character) reacts with NO to generate nitrate [27-32]. These same globins act as nitrite reductases (NiR), which generate NO in the presence of nitrite (NO_2^-) [33-39]. NO-bound Hb (nitrosylHb) can then react slowly in the presence of oxygen to generate nitrate [40]. Interestingly, HSA-heme also behaves as a NiR, [16] which is further confirmed by our lab (vide infra). Importantly, the structural properties of HSA-heme can be tuned to produce effective antioxidant properties. Here, Komatsu and co-workers [22] generated HSA mutants complexed with manganese protoporphyrin IX that displayed superoxide dismutase (SOD) activity, which catalytically scavenges superoxide radical anion. A different native enzyme, catalase, that has a similar Fe(heme)-O(Tyr) bonding interaction as HSA-heme (vide infra), catalytically scavenges and detoxifies peroxynitrite [41]. It is hence conceivable that HSA-heme may have comparable functionality as catalase. In order to gain a better understanding of the function of HSA-heme, its structure must first be established, as described below.

The crystal structure of HSA depicts an all- α chain non-glycosylated protein which contains three domains (I, II, and III) (Figure 1) [42, 43]. Each domain has helical subdomains A and B which are

connected by random protein coils. The binding capabilities of HSA lie within these domains as well as in clefts and polypeptide linkages which connect domains and subdomains. One of the prominent binding regions are the seven areas of fatty acid equivalent binding sites denoted as FA1-FA7 [44]. The FA1 binding site specifically binds an iron heme co-factor, which is stabilized in the connecting loop between subdomains IA

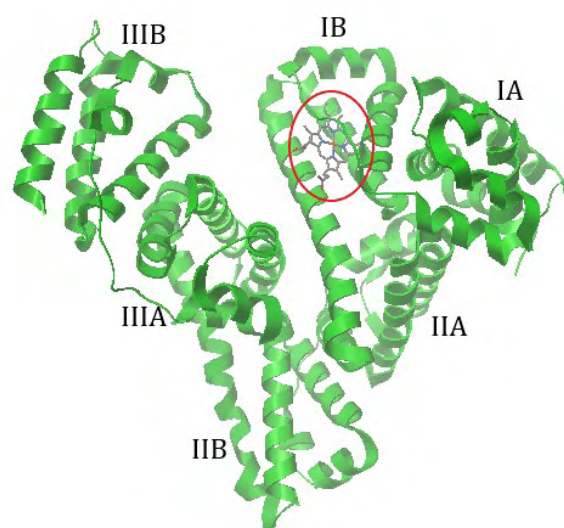


Figure 1. Crystal structure of human serum albumin, HSA-heme (PDB: 1N5U) [26]. The heme *b* co-factor is presented as a stick model (encircled in red). The domains (I-III) and subdomains (A and B) are noted in the structure.

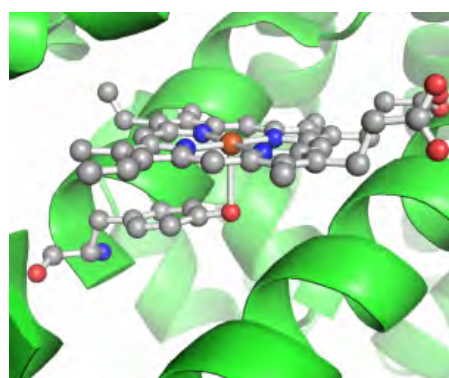


Figure 2. Crystal structure of the FA1 binding site in HSA focusing on the Fe heme *b* (PDB Code: 1N5U) [26]. Heme *b* forms a pentacoordinated complex with Tyr161. The orange, red, blue, and gray spheres represent iron, oxygen, nitrogen, and carbon atoms, respectively.

and IB (Figure 2) [26, 45]. The heme is buried in a hydrophobic cleft where several amino acids show a close interaction with it and appear to play a key role in its binding affinity. These residues are Tyr138, Tyr161, Ile142, His146, and Lys190, which are either conserved or substituted with closely homologous residues in different mammalian serum albumin (SA) [26]. For example, the phenolic oxygen of Tyr161 coordinates to the iron heme 2.73 Å away, generating a weak Fe-O(Tyr) interaction and also forms a hydrogen bonding network with a series of water molecules extending it into a well-defined surface water structure within the hydrophobic cavity. Ile42 provides one of the closest hydrophobic interactions since it is located near the iron on the distal side of the heme. A salt bridge interaction is formed between the propionate groups of the heme and His145 and Lys190. The latter is considered a “gate” residue and is crucial in securing the heme within the hydrophobic cleft. The manipulation of the amino acids in this area allows for effective heme binding, and hence chemistries comparable to native iron heme enzymes such as Hb and Mb [15, 21].

The goal of this study is to understand potential new functions of HSA based on evolutionarily unique amino acids, with particular focus on the residues highlighted above. Here, we investigate SA in several species with different behavioral tendencies (e.g. diving, migration, hibernation) and their ability to utilize oxygen or respond to oxidative stress. We seek to answer the following questions: How has SA been retained throughout mammalian

species? Has evolution retained useful areas of SA such as heme binding or has it denoted new variance to aid with species-specific problems? Here, we present the role of SA in heme binding and oxidative stress in light of existing literature. The information gleaned from these reviews will be utilized to propose new functionalities of SA in various mammalian species based on their amino acid sequence similarities with HSA, with particular focus on oxidative stress response.

MATERIALS AND METHODS

List of species

Data from ten species were collected based on relative similarity with HSA (predominantly mammals), variation in species and living environment, and strains on the species such as potential for oxidative stress (Table 1).

Cross-species analysis

Multiple sequence tool Clustal Omega (version 1.2.4) [46] was used in coordination with the alignment-view program Jalview (version 2.10.3) [47] in order to analyze the amino acid sequence of SA. The protein is compared for properties of conservation, quality, consensus, and occupancy among each amino acid. A coloring functionality was used to allow amino acids with unique properties to be highlighted with various shades according to certain properties like charge, hydrophobicity, size, or propensity to generate a helix. Segments of the alignments from Jalview were included based on

Table 1. GeneBank accession numbers and species assignments for the Serum Albumin (SA) proteins examined in this study.

Animal	Species	Gene	Accession #
Tuatara	<i>Sphenodon punctatus</i>	Serum albumin mRNA, partial cds	AAM46104
Chicken	<i>Gallus gallus</i>	Albumin, mRNA	NP_990592
Chimney swift	<i>Chaetura pelagica</i>	Albumin, mRNA	XP_010001931
Mouse	<i>Mus musculus</i>	Albumin, mRNA	NP_033784
Pig	<i>Sus scrofa</i>	Albumin, mRNA	NP_001005208
Bottlenose Dolphin	<i>Tursiops truncatus</i>	Albumin, mRNA variant X7	XP_019788269
Beluga Whale	<i>Delphinapterus leucas</i>	Albumin, mRNA	XM_022599584
Polar Bear	<i>Ursus maritimus</i>	Albumin, mRNA variant X3	XP_008691428
Human	<i>Homo sapiens</i>	Albumin, mRNA	CAA23754
Weddell Seal	<i>Leptonychotes weddellii</i>	Albumin, mRNA	XP_006729869

the section reviewed, with the full Clustal Omega alignment (Figure 1, SI). Jalview was also used to generate a phylogenetic tree showing relative similarity of proteins based on their sequence. This tree was analyzed along with the protein sequence to further illustrate the relationship between the SA variants.

Preparation of HSA-heme and derivatives

Ferric HSA-heme was prepared according to a previous procedure [48] with some modifications. Here, a solution of 10.7 mg of HSA (Sigma Aldrich) was dissolved in 900 μL phosphate buffer through careful stirring in an ice bath. In a separate preparation, a 800 μL mixture of a 3:5 v/v DMSO/(phosphate/NaCl) buffer was added to 5.8 mg of heme *b* and allowed to mix. The heme *b* (Frontier Scientific) solution was reconstituted into the HSA solution by observing the formation of a Soret band at 404 nm. The heme solution was continuously added until an R/Z ratio of ~ 1.8 was achieved [48]. An R/Z ratio significantly higher than that causes the Soret band to broaden and shift to higher energy, which might indicate the formation of a complex different from the ideal 1:1 heme/HSA. The reconstituted protein was purified through gel filtration using a Sephadex G-50 column (GE Healthcare) that was previously equilibrated with four bed volumes of phosphate buffer.

Ferrous HSA-heme was prepared in a glove box (100% N_2 , Coy Laboratory Products, Inc.) by adding small amounts of sodium dithionite powder to Fe^{III} HSA-heme. The reduction was confirmed by a shift in the Soret band from 404 nm to 415 nm, as previously observed [48]. In order to ensure that HSA-heme remains reduced, a slight excess of the reducing agent was maintained in solution. In producing Fe^{II} -NO HSA-heme, nitric oxide gas (>99% Praxair) was scrubbed through KOH pellets to remove trace quantities of impurities. NO was then bubbled through a previously N_2 -purged phosphate/NaCl buffer, pH 7.4, for several minutes. The saturated NO solution ($\sim 1.7 - 2$ mM [49]) was then added to the Fe^{II} form. Based on this concentration, stoichiometric amounts of NO were added to the Fe^{II} solution to generate the nitrosylated complex. Its formation was monitored *via* a shift in the Soret band from 415 nm to 402 nm.

The NiR reaction of HSA-heme was carried out as follows. Fe^{III} HSA-heme was reduced to the

ferrous form as described above. An anaerobic 100 mM standard solution of nitrite was used as a stock solution. Approximately 40 μL of the nitrite solution was added to ~ 600 μL of 3 μM Fe^{II} HSA-heme, and sealed in an airtight cuvette containing a microstir bar. The changes in the absorption spectrum of the protein were recorded following this reaction.

In order to generate the 1-MeIm HSA-heme complex, Fe^{III} HSA-heme was treated with 40 μL of 1 M 1-methylimidazole in 10 μL additions. In order to create the reduced 1-MeIm HSA-heme complex, Fe^{III} HSA-heme was treated with stoichiometric amounts of sodium dithionite under a nitrogen atmosphere. Forty microliters of 1 M 1-methylimidazole in 10 μL additions were then added to Fe^{II} HSA-heme until a change in the Soret band was observed. The nitrosylated species of Fe^{II} 1-MeIm HSA-heme was generated using a method similar to that described for Fe^{II} -NO HSA-heme (see above).

UV-vis absorption spectroscopy

Absorption measurements were recorded on a Cary 60 double beam UV-vis spectrometer (Agilent Technologies) with a Czerny-Turner monochromator, and a 190-1100 nm wavelength range. Mb and HSA-heme samples were recorded in 100 mM phosphate buffer, pH 7.4, and 25 mM phosphate buffer containing 60 mM NaCl, pH 7.4, respectively.

RESULTS AND DISCUSSION

Heme binding

Heme binds in subdomain IB of HSA, which is the region that is investigated and examined among the species studied. Within this region, five residues play a key role in heme binding: Tyr138, Tyr161, Ile142, His146, and Lys190 [26]. In our work, the amino acid sequence analyses were carried out in the positions comparable to the local alignment within this region in order to study potential similarities in properties of the species studied. It is noted that due to the nature of the Clustal Omega alignment program, which aligns each species based on functionality and amino acid similarity rather than the exact residue number or position, each exact amino acid position is difficult to analyze. To adjust for this, areas near each relevant position in SA are addressed as a whole, and properties in these regions are examined.

The first area that was examined is the hydrophobic adjacent region of Tyr138 in HSA (Figure 3). This region is well-conserved throughout all the mammalian species. Interestingly, it is also conserved in the reptilian species tuatara despite the fact that it is considerably upstream, most likely due to the variation in post translational modification in reptiles compared to mammals. However, in place of Tyr, a slightly more hydrophobic Phe residue is in the location of interest for the bird species investigated. Positions adjacent to this location (before and after respectively) are also well conserved in mammals (all Lys and Leu residues) and show comparable variance in birds (His and Ile) and reptiles (Asn and Ile). Though amino acids in these adjacent positions are not identical, they share the same properties of charge, size, and hydrophobicity, indicating an area of conservation at Tyr138.

The next relative position examined is Ile142 (Figure 4). This region also shows a degree of conservation where the majority of mammals possess Ile with the exception of the mouse, polar bear, and Weddell seal. Coincidentally, each of these species instead has Val, as do both bird

species. Both residues are consistent in property except for size, where the latter is slightly smaller. Regions before and after this residue are also

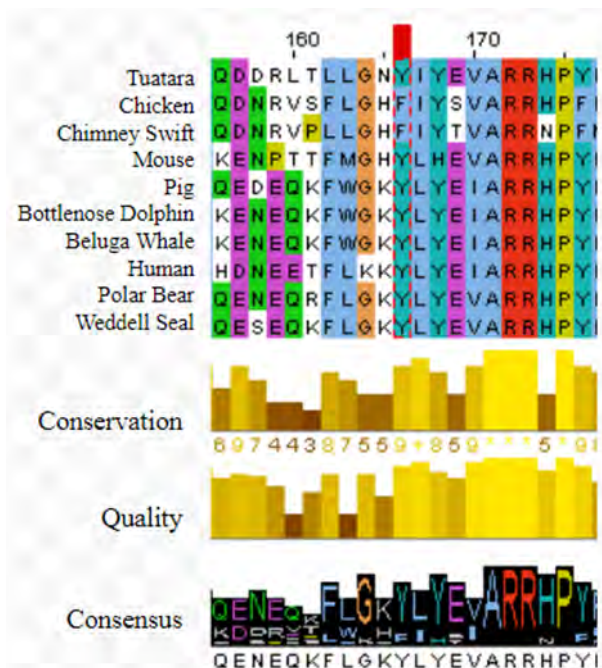


Figure 3. Clustal alignment of 10 species at position 138 with measures of conservation, quality, and consensus.

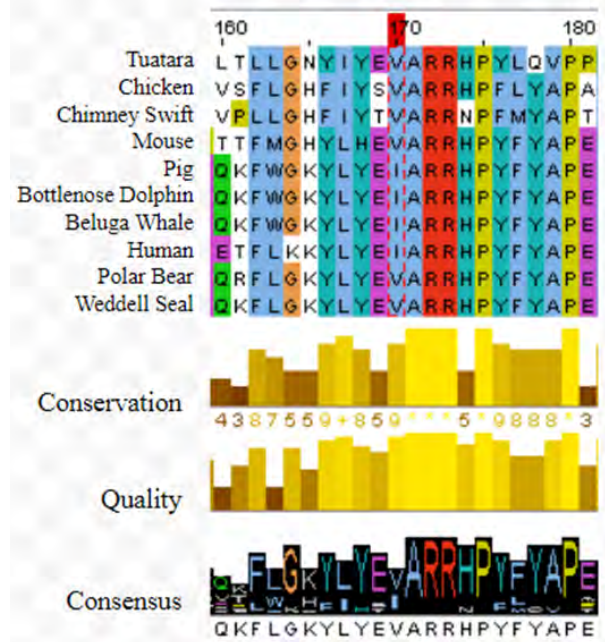


Figure 4. Clustal alignment of 10 species at position 142 with measures of conservation, quality, and consensus.

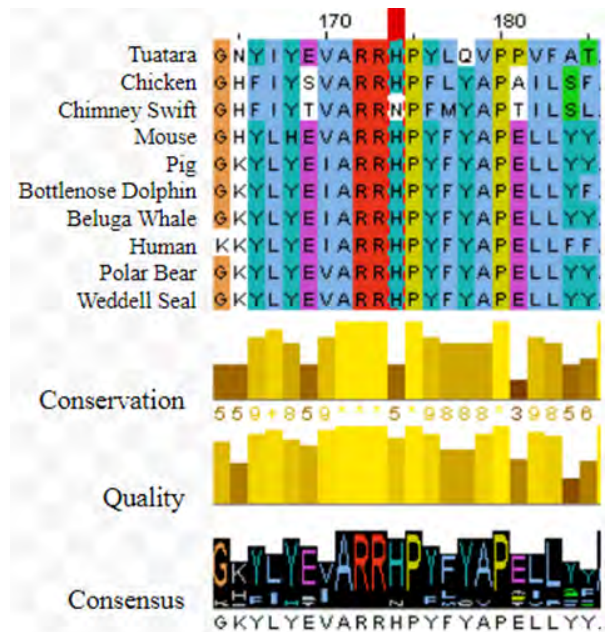


Figure 5. Clustal alignment of 10 species at position 146 with measures of conservation, quality, and consensus.

relatively conserved, as all non-bird species possess a large, negatively charged Glu residue, whereas all species possess Ala. Birds do show a slight variation however, with a very small Ser residue in chickens and a slightly hydrophobic Thr residue in the chimney swift. Both bird species do not have negative residues in this position which may be indicative of heme binding variance.

The following position, His146, is localized in the most conserved region yet (Figure 5). This area is hydrophilic and all species with the exception of the chimney swift contain His at this region. In place of the large, aromatic His residue, the chimney swift contains a small, polar Asn. Despite the species variance one might expect, the positions before and after the His residue are identical in every species, consisting of Arg and Pro, respectively. Evidently the need for a positively charged region prior to, and a small neutral residue after this location is common throughout these species.

Another Tyr residue at position 161 in HSA is related to heme binding in subdomain IB, and also has relative conservation (Figure 6). All species have the Tyr residue excluding the chicken, which contains the hydrophobic and aromatic residue

Phe. Despite the discrepancy, this residue is similar in function to Tyr, except that it lacks polar character. Adjacent regions, however, do show a fairly low similarity. HSA position 160 contains an Arg residue and the comparable region in other species includes Gln in the mouse, bottlenose dolphin, beluga whale, polar bear, and Weddell seal; Asp in the birds; and Leu and Ile in the tuatara and pig, respectively. Gln is relatively inert aside from its polar group, Asp is small, polar, and negative, while Leu and Ile have similar properties to one another. Although the amino acid itself varies, retention in properties is evident except for the hydrophobicity of Leu and Ile. The position following Tyr161 shows similarities, predominantly consisting of Lys save Glu residues in bird species, Asn in mouse, and Asp in the tuatara.

Though Lys190 is deemed a relevant site for heme binding in HSA [26], it is minimally conserved in other species (Figure 7). The most common amino acid in this region is actually Leu, which varies from Lys in charge and aliphatic character. Once again, the chimney swift is unique, possessing a small hydrophobic Ala residue in this position. Despite this variation which is consistent before

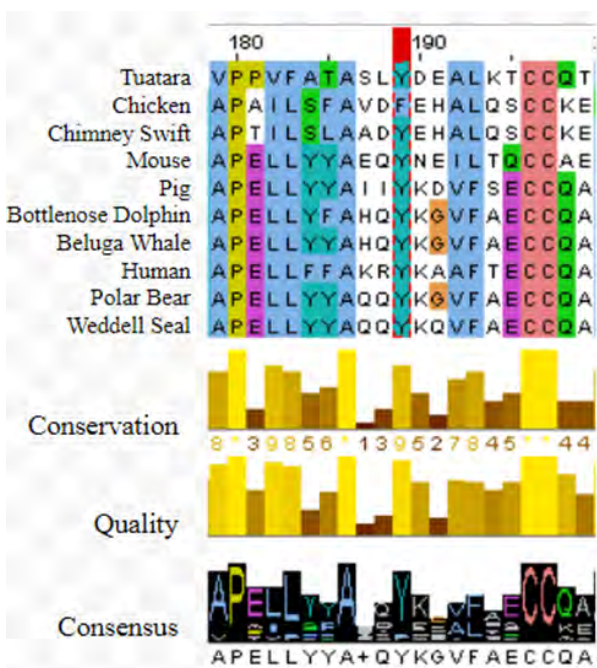


Figure 6. Clustal alignment of 10 species at position 161 with measures of conservation, quality, and consensus.

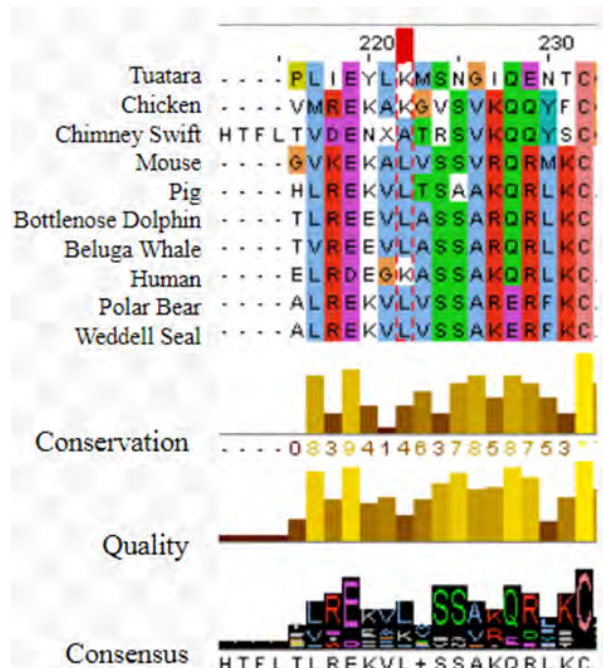


Figure 7. Clustal alignment of 10 species at position 190 with measures of conservation, quality, and consensus.

and after position 190, this region is a largely hydrophobic area, indicating the propensity for the formation of a hydrophobic binding pocket.

Although the amino acid sequence for each species is not in exact alignment, the clustal alignment by function shows a clear similarity at key heme interaction sites in HSA. If these regions do not share the exact amino acid, they often possess a residue with a very similar size, charge, structure, or hydrophobicity. Each of the five binding regions showed high similarity across each species, with conservation values consistently ~90%. Conservation throughout the protein is fairly prominent, often reaching values of 80% or higher. The first 50 amino acids, which is often a site of species specific protein modification, show low conservation as one might expect. The tuatara is represented as a blank in this region, starting alignment much farther down the protein sequences of other species (residue 161 in HSA for example, is only 82 in the tuatara). Since the tuatara was chosen as an outlier due to its genetic difference from mammals and unique variation from birds, it is not surprising that this area is different to the point of nonexistence. Based on this protein similarity, or lack thereof, Jalview is able to generate phylogenetic trees with or without relative branch distances. These trees are outlined in Figure 8. Although the function of SA regions may be conserved between species, each tree is generated solely based on amino acid similarity. As expected, the tuatara was an outgroup with less relative similarity to the rest of the mammals. In addition, the unique clade of bird species was most similar to the tuatara. Aside from this, each mammalian species showed short branch lengths and decent similarity. A particular closeness was observed between the bottlenose dolphin and beluga whale, and the polar bear and Weddell seal as these pairs are both clades based on protein similarity.

The relevant regions outlined by Carter and co-workers [26] and Komatsu *et al.* [21] do seem to be relatively conserved throughout species at least in the properties of the amino acids. This retention of function may indeed suggest that conservation of these regions is evolutionarily beneficial, and the propensity for SA to bind heme may potentially have some impact on oxidative stress correction. To examine this possibility, the next section will

focus on blood chemistry of organisms with oxidative stress. These include the stresses of behavioral tendencies such as hibernation, migration, and sea diving.

Oxidative stress

In order to support the notion of SA's function in handling oxidative stress, one must consider the blood chemistry of species which accommodate such stress and possible mechanisms of doing so. Though most of these mechanisms relate to modulation of metabolic rate and careful regulation of various enzymes and antioxidants, the function of such mechanisms could shed light on the potential role of SA as an accommodating factor. Though each species in the alignment analysis will not be individually examined for stress accommodation, species with similar physiology which have the same behavioral tendencies (diving, migration, hibernation) will be used as models.

When analyzing the possible routes of handling oxidative stress, it is important to recognize that oxidative stress may exist for a variety of different reasons, and many corrective pathways exist besides increasing oxygen carrying ability. In most species, it is not only a lack of oxygen (anoxia) which is associated with oxidative stress, but the influx of ROS and RNS once an individual re-enters an oxygen rich environment [50]. Three predominant ways to deal with oxidative stress may include preventing ROS and RNS formation, using free radical scavengers or antioxidant enzymes, and repairing damaged cellular components. SA could be affiliated with two of these options, preventing ROS formation by aiding in oxygen transport or using its inherent scavenging ability to neutralize ROS and RNS [23, 24].

A large group of mammals analyzed (such as the bottlenose dolphin, beluga whale, Weddell seal, and polar bear) face a sizeable amount of oxidative stress when deep sea diving. Vazquez-Medina and co-workers [51] examined this stress in deep-sea diving hooded seals. Seals have a physiological reaction equivalent to the mammalian diving reflex in humans, characterized by vasoconstriction in the periphery and slowed heart rate (bradycardia) to minimize oxygen consumption. However, it seems as though the biggest challenge of anoxia is the presence of ROSs and overall oxidative damage,

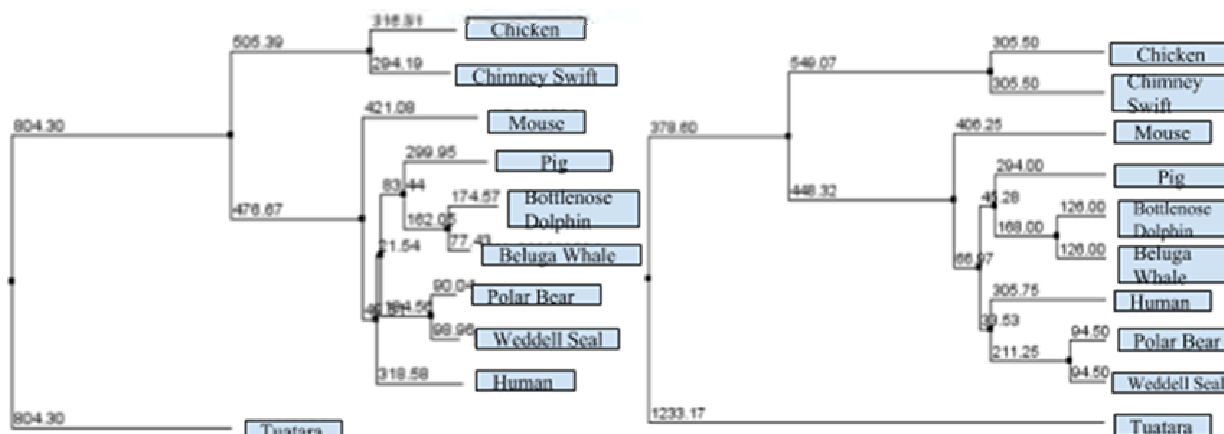


Figure 8. Phylogenetic tree of each analyzed species with relative branch lengths.

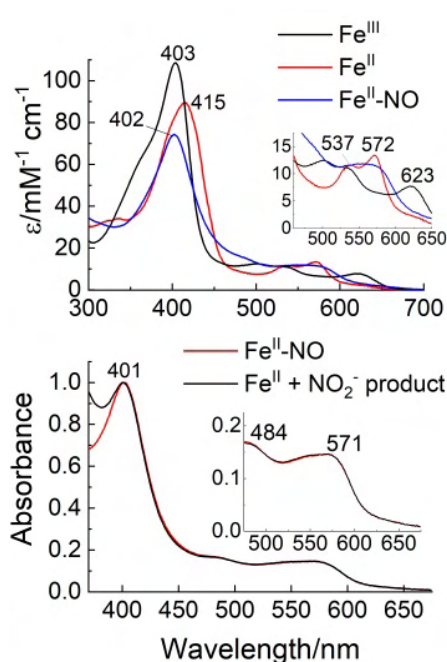


Figure 9. Top: UV-visible absorption spectra of HSA-heme Fe^{III} (black line), Fe^{II} (red line), and $\text{Fe}^{\text{II}}\text{-NO}$ (blue line). $10.9 \mu\text{M}$ of Fe^{III} was used prior to reduction and reaction with NO or NO_2^- . Bottom: Overlay of the normalized absorption spectra of HSA-heme $\text{Fe}^{\text{II}}\text{-NO}$ (red line) and the product of the reaction between Fe^{II} and NO_2^- (black line). Absorption spectra were recorded in 25 mM phosphate buffer containing 60 mM NaCl, pH 7.4.

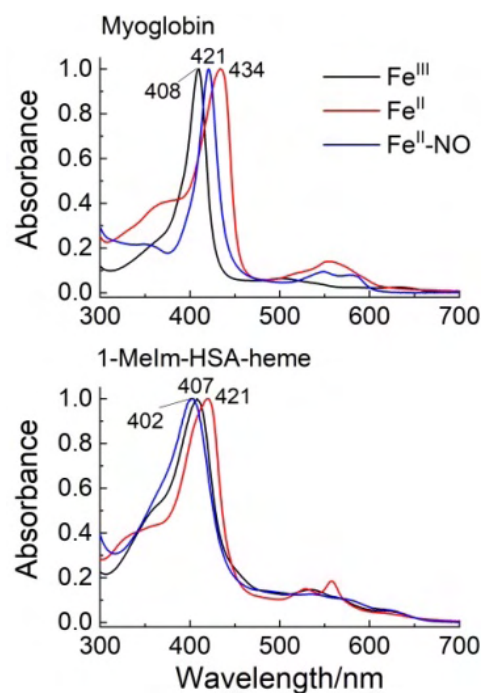


Figure 10. UV-visible absorption spectra of myoglobin (top) and 1-MeIm-HSA-heme (bottom) showing the different forms of the enzyme as Fe^{III} (black line), Fe^{II} (red line), and $\text{Fe}^{\text{II}}\text{-NO}$ (blue line). Absorption spectra were recorded in 100 mM phosphate buffer, pH 7.4 (myoglobin), and 25 mM phosphate buffer containing 60 mM NaCl, pH 7.4 (1-MeIm-HSA-heme).

therefore making an increase in antioxidant production as the most prevalent protective factor. Antioxidants consist of enzymatic and non-enzymatic species such as enzymatic SOD, catalase, glutathione

peroxidases, and peroxiredoxins, and non-enzymatic glutathione (GSH) [51]. In addition to antioxidants, Vazquez-Medina and co-workers [51] also discovered that there is a transcription factor, Nrf2,

which up-regulates the production of these enzymatic antioxidants in diving mammals. Although these protective mechanisms are not associated with oxygen carrying ability, the need for oxygen transport and ROS/RNS binding would still likely be necessary in these species. For this reason, it is not unrealistic to think that a retention of this functionality in SA would be evolutionarily selected in diving mammals. An explanation for this is provided below.

Other sources of oxidative stress are associated with the variations in blood flow during hibernation (which is seen in pregnant female polar bears), and the high activity and low oxygen concentrations seen in migration. Carey and co-workers [52] examined a model of hibernation in ground squirrels. Once again, a focus is placed on the activation of oxidative stress pathways rather than oxygen carrying efficiency. Here, another transcription factor, NF- κ B, is redox sensitive and alters regulation of antioxidant enzymes in concert with the stress prevalent protein GRP75 [52]. This method has also been mimicked in migratory birds as described by Cooper and co-workers [52]. The predominant source of dealing with oxidative stress is accommodating reactive (oxygen or nitrogen) species, and this is done by endogenous antioxidant increase or a dietary increase in antioxidants [52]. For example, within the blood, there is a clear antioxidant effect of GSH similar to what is seen in diving mammals. In addition, uric acid and SOD3 function as antioxidants in the blood plasma and are unique to birds and other uricotelic organisms. Based on this, these species may use this physiological component to adjust for oxidative stress rather than a unique form of SA. Despite this, birds (both migratory and non-migratory) and reptiles included in the clustal alignment have areas of conservation similar to HSA and other mammals.

While the mode of oxidative stress response of the species described above does not directly utilize SA, this protein can behave as an antioxidant. In humans, SA provides high affinity sites for Cu^{II} and Fe^{II} , limiting the damage created by these ions when hydroxyl radicals are produced *via* the Fenton reaction [23, 53, 54]. HSA also has free radical trapping properties, as it uses the free thiol in the Cys34 residue to scavenge ROS and RNS [24, 55]. Beyond native HSA, the heme bound

complex, HSA-heme, functions as a NiR,[16] and binds NO [56]. A UV-vis spectral profile depicting the NiR activity of HSA-heme is presented in Figure 9. Here, the NiR activity of HSA-heme was tested by adding NO_2^- to the reduced form of the heme (Fe^{II}). Dithionite was used to reduce Fe^{III} (403 nm) to Fe^{II} (415 nm) and was kept in slight excess to prevent its re-oxidation. Addition of NO_2^- to the faint yellow HSA-heme Fe^{II} solution shifts the Soret band from 415 nm to 402 nm, producing a peach-colored solution. The observed trend in the shift of the Soret band (from low to high energy upon addition of NO_2^-) is consistent with Mb Fe^{II} [34]. In order to deduce the identity of the product, the absorption spectrum generated from a pure Fe^{II} -NO species, also a peach-colored solution, was overlaid and normalized with that obtained from the reaction product of HSA-heme Fe^{II} and NO_2^- . As shown in the bottom of Figure 9, the features in both spectra match very well, which strongly suggest the formation of NO through NO_2^- reduction. In both spectra, the Soret band occurs at 401 nm, while the lower energy Q-region displays a broad peak with a subtle shoulder at 571 and 550 nm, respectively, and a weak feature at 484 nm. Since dithionite is present in slight excess in solution, the final product is expected to only be Fe^{II} -NO. It is conceivable that HSA-heme may potentially detoxify NO through an oxygen-mediated oxidation of Fe^{II} -NO, similar to that observed in Hb [40]. To our knowledge, the latter process has not been conclusively verified but preliminary electrochemical tests on HSA-heme and Mb (that have properties similar to Hb) indicate comparable catalytic reduction in the presence of NO_x species (data not shown).

Aside from detoxifying NO, HSA-heme may potentially scavenge peroxynitrite using a mechanism similar to catalase, which also has a Fe-O(Tyr) bonding interaction. Catalase reacts with ONOO^- to form a catalase-peroxynitrito complex, which decays to either catalase directly or *via* compound II [41]. Here, Gebicka and co-worker suggest that catalase may be part of a defense mechanism against peroxynitrite when the pH is lowered and when present in tissues with high expression of this enzyme. Notably, the residue proximal to the heme that binds directly to the Fe center (e.g. phenolate from Tyr in the case of HSA-heme and catalase)

plays a key role in the reactivity of ligands bound to the metal [57-60]. For example, adding 1-methylimidazole (1-MeIm, a small ligand that resembles His) to HSA-heme forms a complex that generates spectral features that have relative shifts comparable to Mb (a protein with a proximal His) but are distinctly different from native HSA-heme (Figures 9 and 10). This complex, 1-MeIm-HSA-heme, presumably forms a Fe-N(1-MeIm) bonding interaction similar to that observed when 2-methylimidazole is added to HSA-heme [48]. The Soret band of the oxidized Fe^{III} species (408 nm for Mb; 407 nm for 1-MeIm-HSA-heme) shifts to lower energy upon reduction to Fe^{II} (434 nm for Mb; 421 nm for 1-MeIm-HSA-heme). Incorporation of NO to the reduced form (Fe^{II}-NO) then shifts the Soret band back to higher energy in both enzymes. This underscores the importance of the proximal ligand in controlling the reactivity of the heme enzyme, and alludes to the possibility of HSA-heme to function as a peroxynitrite scavenging species as described above. It is noteworthy that beyond the residue proximal to the heme plane, the distal residues also play a role in heme enzyme reactivity and would be worthwhile to explore in future studies for HSA-heme [61-63].

Ultimately, methods of coping with oxidative stress seem to focus less on oxygen carrying manipulation, and more on the accommodation of reactive species which are generated in hypoxic conditions or a return from these conditions. Regions that allow for heme binding in HSA are retained with an exact amino acid or similar function across species, and potentially appear to be a factor in oxidative stress accommodation when considering functions of other heme

enzymes. Definitive analysis of SA-heme as a free radical scavenger is more useful in correlating oxidative stress across species. Based on our results, the structural variation or conservation in SA across each species may be linked with the physiological traits of these species, in particular, oxidative stress related to the presence of heme.

CONCLUSION

The amino acids within subdomain IB of HSA that are crucial in coordinating heme are fairly conserved among the species investigated, indicating this region to be evolutionarily valuable with respect to this heme binding function. Heme enzymes such as globins and catalase utilize its active site to scavenge and detoxify ROS and RNS, and given parallel functional and structural similarities with HSA-heme, it is plausible that the latter also uses this co-factor in oxidative stress response. Given its propensity to bind NO_x species such as nitric oxide, the utility of HSA-heme to attenuate NO signaling (beyond preventing NO toxicity) is also an interesting concept. More studies will need to be carried out to verify this idea.

ACKNOWLEDGEMENTS

S. A and A. A. C. would like to thank Penn State Behrend Undergraduate Research Grant Programs for funding. M. G. I. G. would like to thank previous research students Kevin Kang and Christopher D. Kimrey for preliminary work done on the spectral analysis of the NiR reaction of HSA-heme, and the different forms of HSA-heme imidazole complexes, respectively.

SUPPORTING INFORMATION

Clustal omega alignment multiple sequence alignment for different species.

Figure 1. Clustal Omega (1.2.4) multiple sequence alignment for the ten species investigated in this work. The SA sequence number for each species is listed in the first column.

```

AAM46104 ----- 0
NP_990592 MKWVTLISFIFLFFSSATSRNLQRFARDAEHKSEIAHRYNDLKEETFKAVAMITFAQYLQR 60
XP_010001931 MKWVTLISFIFLFFSSATSRNLQRVARGAEHKSEIAHRYNDLKEETFKAVMTITFAQYLQR 60
NP_033784 MKWVTFLLLLFVSGSAFSGVVF---RREAHKSEIAHRYNDLGEQHFKGLVLI AFSQYLQK 57
NP_001005208 MKWVTFISLLFLFSSAYSARGVF---RRDTYKSEIAHRFKDLGEQYFKGLVLI AFSQHLQQ 57
XP_019788269 -----MTCSAYSARGVF---RRDTHKSEIAHRFNLDGEEFNFKGLVLI AFSQYLQQ 46
XM_022599584 MKWVTFISLIFLFFSSAYSARGVF---RRDTHKSEIAHRFNLDGEEFNFKGLVLI AFSQYLQQ 57
CAA23754 MKWVTFISLLFLFSSAYSARGVF---RRDAHKSEVAHRFKDLGEEFNKALVLI AFAQYLQQ 57
XP_008691428 MKWVTFISLLFLFSSAYSARGVT---RREAQQSEIAHRYNDLGEEHFRGLVLI AFSQYLQQ 57
XP_006729869 MKWVTFISLLFLFSSAYSARGVM---RREAQQSEVAHRYNDLGEEHFRGLVLI AFSQYLQQ 57

```

Figure 1 continued..

AAM46104	-----EDPTCLKSLDTIFLDEICHEEGFAAKYD-LAACCAK	35
NP_990592	CSYEGLSKLVKDVVDLAQKCVANEDAPECSKPLPSIILDEICQVEKLRDSYGAMADCCSK	120
XP_010001931	CSYEGLSKLVKDVVDLAQKCVADEAAGCSKPLPSIFLDEICQVEKLRDSYGAMADCCSK	120
NP_033784	CSYDEHAKLVQEVTDFAKTCVADESAANCDKSLHTLFGDKLCAIPNLRENYGELADCCTK	117
NP_001005208	CPYEEHVKLVREVTEFAKTCVADESAENCDKSIHTLFGDKLCAIPSLREHYGDLADCCEK	117
XP_019788269	SPFDEHVKLVNEITDFAKTCVADESAANCDKSLHTLFGDKLCAVASLRETYGEMADCCGK	106
XM_022599584	SPFDEHVKLVNEITDFAKTCVADESATNCDKSLHTLFGDKLCAVASLRETYGEMADCCVK	117
CAA23754	CPFEDHVKLVNEVTEFAKTCVADESAENCDKSLHTLFGDKLCTVATLRETYGEMADCCAK	117
XP_008691428	CPFEDHVKLAKEVTEFAKGCADQSGADCDKSLHTLFGDKLCTVASLREKYGELADCCEK	117
XP_006729869	QDPERNECFLTHKDDNPGF-PPLVTPPEPDAMCAAFQSEQKFLGKYLVEVARRHPYFYAP	117
	. * * : : : * : * : * . : * * * *	
AAM46104	AEVERKECLLAHKNATPGFIPAFQRPGLIEVSKLYQDDRLTLLGNYIYEVARRHPYLQVP	95
NP_990592	ADPERNECFLSFKVSPDFVQPYQRPASDVICQEYQDNRVSFGLGHFIYSVARRHPFLYAP	180
XP_010001931	ADPERNDCFLSFKIPQPDFVPPYERSSDVICKEYQDNRVPLLGHFIYTVARRNPFMYAP	180
NP_033784	QEPERNECFLQHKDDNPSL-PPFERPEAEAMCTSFKENPTTFMGHYLHEVARRHPYFYAP	176
NP_001005208	EPPERNECFLQHKDDNPDPI-PKL-KPDPVALCADFQEQKFWGKYLVEIARRHPYFYAP	175
XP_019788269	QDPERNECLLKHKDDNPDL-PKL-KPDPETFCTEFKENEQKFWGKYLVEIARRHPYFYAP	164
XM_022599584	QEPERNECLLKHKDDNPDL-PKL-KPDPDTLCAEFKENEQKFWGKYLVEIARRHPYFYAP	175
CAA23754	QEPERNECFLQHKDDNPNL-PRLVLRPEVDVMCTAFHDNEETFLKKYLVEIARRHPYFYAP	176
XP_008691428	QEPERNECFLKHKDDNPGF-PPLVTPPEPDALCAAFQENEFKYLVEVARRHPYFYAP	176
XP_006729869	QDPERNECFLTHKDDNPGF-PPLVTPPEPDAMCAAFQSEQKFLGKYLVEVARRHPYFYAP	176
	: * * : * * . * * : * . * : : : : * : * * * * : *	
AAM46104	PVFATASLYDEALKTCCTADKATCFHPRIP----PLIEYLKMSNGIQENTCGILKKFGE	151
NP_990592	AILSFAVDFEHALQSCCKESDVGACLDTKIEI---VMREKAKGVSVKQQYFCGILKQFGD	236
XP_010001931	TILSLAADYEHALQSCCKEADVNAACLDKVVHHTFLTVDENXATRSVKQQYSCGILQKFGGE	240
NP_033784	ELLYYAEQYNEILTQCCAADKESCLTPKLD---GVKEKALVSSVRQRMKCSMQKFGGE	232
NP_001005208	ELLYYAIYKDVSECCQAADKAACLIPKIEI---HLREKVLTSAAKQRLKCSIQKFGGE	231
XP_019788269	ELLYFAHQYKGVFAECCQAADKGAACLIPIKIEI---TLREEVLASSARQRLKCTSIQKFGGE	220
XM_022599584	ELLYYAHQYKGVFAECCQAADKGAACLIPIKIEI---TVREEVLASSARQRLKCTSIQKFGGE	231
CAA23754	ELFFAKRYKAAFTQCCQAADKAACLIPKLD---ELRDEGKASSAKQRLKCASLQKFGGE	232
XP_008691428	ELLYYAQQYKGVFAECCQAADKAACLIPKID---ALREKVLVSSARERFKCASLQKFGD	232
XP_006729869	ELLYYAQQYKGVFAECCQAADKAACLIPKID---ALREKVLVSSAKERFKCASLQKFGD	232
	: : * : . : * * : * : * : : : : . * : * * * :	
AAM46104	RTLKATKLVQMSQKFPKADFATINKLVEDITHMTECCRGDTLECLRDREALTEYTCCHK	211
NP_990592	RVFQARQLIYLSQKYPKAPFSEVSKFVHDSIGVHKECCEGDMVECDMDMARMMSNLCSQQ	296
XP_010001931	RIFKAQKLAIMSQKYPKAPLTELKVVVNDIHKKECCSGDMVECDMDRAELVTVICSKQ	300
NP_033784	RAFKAWAVARLSQTFPNADFAEITKLATDLTKVNKECCHGDLLCADDRADLAKYMCENQ	292
NP_001005208	RAFKAWSLARLSQRFPKADFTEISKIVTDLAKVHKECCHGDLLCADDRADLAKYICENQ	291
XP_019788269	RALKAWSVARLSQKFPKADFAEVSKIIVTDLTKVHKECCHGDLLCADDRADLAKYICENQ	280
XM_022599584	RALKAWSVARLSQKFPKADFAEVSKIIVTDLTKVHKECCHGDLLCADDRADLAKYICENQ	291
CAA23754	RAFKAWAVARLSQRFPKAEFAEVSKLVTDLTKVHTECCHGDLLCADDRADLAKYICENQ	292
XP_008691428	RAFKAWSVARLSQRFPKADFAEVSKVVTDLTKVHKECCHGDLLCADDRADLAKYMCENQ	292
XP_006729869	RAFKAWSIALMSQKFPKADFAEVSKLVTDLTKIHKECCHGDLLCADDRADLAKYMCENQ	292
	* : * : : * * : * * : : : * . * : : * * * * * * * : * : :	
AAM46104	DAISSKLPCCCEKSVLERGECIVRLENDKPADLSERIAEYIEDPHVCDHLAKEQDAFLA	271
NP_990592	DVFSGKIKDCCEKPIVERSQCIMEAEFDEKPADLPSLVEKYIEDKEVCKSFQAGHDAFMA	356
XP_010001931	DVFSKIKKECCEKPVVERSQCIESEYDDKPEDLPSLVEKYVQDKEVCNGFQKDHGDFMS	360
NP_033784	ATISSKLTCCDKPLLKKAHCLSEVEHDTMPADLPAIAADFVEDQEVCKNYAEAKDVFLG	352
NP_001005208	DTISTKLKECCDKPILLEKSHCIAEAKRDELPAADLPLEHDFVEDKEVCKNYEAKHVFLG	351
XP_019788269	ATISSKLQKCKPILLEKSHCISEVEKDELPELNSLLAADFAEDKEVCKNYEAKDVFLG	340
XM_022599584	ATISTKLKCCDKPILLEKSHCIAEVEKDELPELNSPLAADFAEDKEVCKNYEAKDVFLG	351
CAA23754	DSISSKLECCDKPILLEKSHCIAEVENDEMPADLPSLAADFVESKDVCKNYEAKDVFLG	352
XP_008691428	DSISSKLECCDKPVLKESQCLSEVERDELPGDLPLAADFVEDKEVCKNYEAKDVFLG	352
XP_006729869	DSISSKMECCDKPILLEKSHCLTEVERDELPGDLSPIAADFVEDKEVCKNYEAKDVFLG	352
	: * * : * * . * : : : . * : : * * * * * : : . * * . : * :	
AAM46104	KFLYEYSRRHPPELSTQILLGVGKGYQELLERCCCKTDNPPCEYGAQAEADLKKHIAQFQELV	331
NP_990592	EFVYEYSRRHPEFSIQLIMRIAKGYESLLEKCKCKTDNPAECYANAQEQLNQHIKETQDVV	416

Figure 1 continued..

XP_010001931	EFLYEYSRRHPEFSTQLILRIAKGYEALLEKCKTDNPAECYGNAQEELNKHVQETQEVV	420
NP_033784	TFLYEYSRRHPDYSVSLLLRLAKKYEATLEKCCAEANPPACYGTVLAEFQPLVVEEPKNLV	412
NP_001005208	TFLYEYSRRHPDYSVSLLLRIAKIYEATLEDCCAKEDPPACYATVFDKFQPLVDEPKNLI	411
XP_019788269	TFLYDYARRHPEYSVSLLLRIAKGYEATLEDCCAKDDPPACYATVFEKLRPLVEEPKNLI	400
XM_022599584	TFLYDYARRHPEYAVSLLLRRIAKGYEATLEDCCAKDDPPACYATVFEKLRPLVEEPKNLI	411
CAA23754	MFLYDYARRHPDYSVLLLRRLAKTYETTLKCCAAADPHECYAKVFDEFKPLVEEPQNLII	412
XP_008691428	TFLYEYSRRHPEYSVSLLLRLAKEYEATLEKCCATDDPPTCYSKVLDEFKPLVEEPQNLV	412
XP_006729869	TFLYEYSRRHPEYAISSLLLRRLAKEYEATLEKCCATDDPPTCYGKVLDEFKPLVEEPQNLV	412
	*:::****: : :: : . * * : * * * : * * . . . : : : : :	
AAM46104	QQNCDLYNTLGGYLFHNNALLIRYTKRMPQLTSEELIFYT-RITKAASRCCEVSVDKLLPC	390
NP_990592	KTNCDLLHDHGEADFLKSILIRYTKKMPQVPTDLLLETGKMTTIGTKCCQLPEDRRMAC	476
XP_010001931	KTNCELLNTHGEADFLKSLIRYTKKMPQVSTETLLEIGKKMSTVGTKCCQLPEDRRLPC	480
NP_033784	KTNCDLYEKLGEYGFQNALIVRYTQKAPQVSTPTLVEAARNLGRVGTCCCTLPEDQRLPC	472
NP_001005208	KQNCLEFKEKLGEYGFQNALIVRYTKKVPQVSTPTLVEVARKLGLVGSRCCKRPEEERLSC	471
XP_019788269	KQNCLEFKEKLGEYGFQNALIVRYTKKVPQVSTPTLVEVSRNLGRVGSCKCKNPESERMSC	460
XM_022599584	KQNCLEFKEKLGEYLFQNALIIRYTKKVPQVSTPTLVEVSRNLGRVGSCKCKNPESERMSC	471
CAA23754	KQNCLEFKQLGEYKFNALLVRYTKKVPQVSTPTLVEVSRNLGKVGSKCKKHPEAKRMP	472
XP_008691428	KSNCELFKEKLGEYAFQNALIVRYTKKVPQVSTPTLVEVSRNLGKVGTKCKCKNPESERMSC	472
XP_006729869	KTNCLEFKEKLGEYGFQNALIVRYTKKVPQVSTPTLVEVSRNLGKVGTRCCKKPDSEMRPC	472
	: **:* . * * : : : : ****: : ** : * : . : : ** . : : *	
AAM46104	TEGYVDFVLGQICQRHQSSINNVNVCQCCSNSYALRSLCITSLGGDEKVFVPIEFSADLFT	450
NP_990592	SEGYLSIVIHDTCRKQETTPINDNVSQCCSSSYANRRPCFTAMGVDTKYVPPFPNPMFS	536
XP_010001931	SEGYLSIVIQDMCRRQETTPINDNVSQCCSNSYADRRCFTKMGVDTKYVPPAFDPNMFN	540
NP_033784	VEDYLSAILNVRVCLLHEKTPVSEHVTCCSGSLVERRPCFSALTVDETYVPKEFKAETFT	532
NP_001005208	AEDYLSLVNRLCVLHEKTPVSEKVTCCCTESLVNRRPCFSALTPDETYKPKFEVGTFT	531
XP_019788269	AEDYLSLVNRLCVLHEKTPVSEKVTCCCTESLVNRRPCFSALTVDETYKPKAFDEKFTFT	520
XM_022599584	AEDYLSLVNRLCVLHEKTPVSEKVTCCCTESLVNRRPCFSALTVDETYKPKAFDEKFTFT	531
CAA23754	AEDYLSVVLNQLCVLHEKTPVSDRVTKCCTESLVNRRPCFSALVDETYVPKEFNAETFT	532
XP_008691428	AEDYLSVVLNRLCVLHEKTPVSEKVTCCCTESLVNRRPCFSALVDETYVPKEFNAETFT	532
XP_006729869	AEDYLSVVLNRLCVLHEKTPVSEKVTCCCTESLVNRRPCFSALVDETYVPKEFNAETFT	532
	*. * . : : * : : : . * : * : * * : : * : * * *	
AAM46104	FHEDLCHAAQDKLQERKQQMIVNLVKHKPNITKEQLQTVFGGFTKMTEKCKAEDHEACF	510
NP_990592	FDEKLCSAPAEEREVGQMKLLINLIKRPQMTEEQIKTIADGFTAMVDKCKQSDINTCF	596
XP_010001931	FDEKLCSASPAEQELGQMKLLINLIKRPQMTEEQIKTIADGFTAMVDKCKQADIETCL	600
NP_033784	FHSDICTLPEKEKQIKKQATALAELVKHKPKATAEQLKTVMDDFAQFLDTCCKAADKDTCF	592
NP_001005208	FHADLCTLPEDKQIKKQATALVELLKHKPHATEEQLRVTLGNFAAFVQKCCAAPDHEACF	591
XP_019788269	FHADLCTLPENKQIKKQIALVELVKHKPKVTEEQKLTVMGDFAAFVQKCCAADDKEACF	580
XM_022599584	FHADLCTLPENKQIKKQIALVELVKHKPKVTEEQKLTVMGDFAAFVQKCCAADDKEACF	591
CAA23754	FHADICTLSEKERQIKKQATALVELVKHKPKATKEQLKAVMDDFAAFVEKCKADDKETCF	592
XP_008691428	FHADLCTLPAAEQAKKQSALVELLKHKPKATEEQKLTVMGDFGAFVQKCCAENKEGCF	592
XP_006729869	FHADLCTLPAAEQVKKQSALVELVKHKPKATEEQKLTVMGDFGAFVEKCCAENKEACF	592
	* . : * : : : : * : * : * : * : * : * : * : *	
AAM46104	GEEGPKLVAESQTALAA-- 527	
NP_990592	GEEGANLIVQSRATLGIGA	615
XP_010001931	GEEGANLIVQGRAILGIGM	619
NP_033784	STEGPNLVTRCKDALA---	608
NP_001005208	AVEGPKFVIEIRGILA---	607
XP_019788269	ALEGPKLVVKTREAIA---	596
XM_022599584	ALEGPKLVVSTREAIA---	607
CAA23754	AEEGKLVVAASQAALGL-- 609	
XP_008691428	AEEGPKLVATAQAALV---	608
XP_006729869	AEEGPKLVAKAQAALA---	608
	. ** : : : :	

Note: “.” denotes large variance, “:” denotes small variance, and “*” denotes high conservation.

CONFLICT OF INTEREST STATEMENT

The authors declare no competing financial interest.

REFERENCES

1. Bertucci, C. and Domenici, E. 2002, *Curr. Med. Chem.*, 9, 1463.
2. Iqbal, M. J., Dalton, M. and Sawers, R. S. 1983, *Clin. Sci. (Lond.)*, 64, 307.
3. Bal, W., Sokolowska, M., Kurowska, E. and Faller, P. 2013, *Biochim. Biophys. Acta*, 1830, 5444.
4. Haeri, H. H., Schunk, B., Tomaszewski, J., Schimm, H., Gelos, M. J. and Hinderberger, D. 2019, *ChemOpen*, 8, 650.
5. Curry, S., Brick, P. and Franks, N. P. 1999, *BBA - Mol. Cell Biol. L.*, 1441, 131.
6. Ascenzi, P., Bocedi, A., Notari, S., Fanali, G., Fesce, R. and Fasano, M. 2006, *Mini Rev. Med. Chem.*, 6, 483.
7. Leboffe, L., di Masi, A., Trezza, V., Polticelli, F. and Ascenzi, P. 2017, *IUBMB Life*, 69, 834.
8. Sendzik, M., Pushkie, M. J., Stefaniak, E. and Haas, K. L. 2017, *Inorg. Chem.*, 56, 15057.
9. Kamal, J. K. and Behere, D. V. 2005, *Indian J. Biochem. Biophys.*, 42, 7.
10. Adams, P. A. and Berman, M. C. 1980, *Biochem. J.*, 191, 95.
11. Froehlich, E., Mandeville, J. S., Jennings, C. J., Sedaghat-Herati, R. and Tajmir-Riahi, H. A. 2009, *J. Phys. Chem. B*, 113, 6986.
12. Rozga, J., Piatek, T. and Malkowski, P. 2013, *Ann. Transplant*, 18, 205.
13. Fanali, G., Di Masi, A., Trezza, V., Marino, M., Fasano, M. and Ascenzi, P. 2012, *Mol. Aspects Med.*, 33, 209.
14. Ohnishi, K., Kawaguchi, A., Nakajima, S., Mori, H. and Ueshima, T. 2008, *J. Clin. Pharmacol.*, 48, 203.
15. Komatsu, T., Nakagawa, A., Zunszain, P. A., Curry, S. and Tsuchida, E. 2007, *J. Am. Chem. Soc.*, 129, 11286.
16. Ascenzi, P., Tundo, G. R., Fanali, G., Coletta, M. and Fasano, M. 2013, *J. Biol. Inorg. Chem.*, 18, 939.
17. Ascenzi, P., di Masi, A., De Sanctis, G., Coletta, M. and Fasano, M. 2009, *Biochem. Biophys. Res. Commun.*, 387, 83.
18. Ascenzi, P., Cao, Y., Di Masi, A., Gullotta, F., De Sanctis, G., Fanali, G., Fasano, M. and Coletta, M. 2010, *FEBS Journal*, 277, 2474.
19. Sakurai, Y., Ma, S. F., Watanabe, H., Yamaotsu, N., Hirono, S., Kurono, Y., Kragh-Hansen, U. and Otagiri, M. 2004, *Pharm. Res.*, 21, 285.
20. Watanabe, K., Ishikawa, N. and Komatsu, T. 2012, *Chem. Asian J.*, 7, 2534.
21. Komatsu, T., Ohmichi, N., Nakagawa, A., Zunszain, P. A., Curry, S. and Tsuchida, E. 2005, *J. Am. Chem. Soc.*, 127, 15933.
22. Kato, R., Kobayashi, Y., Akiyama, M. and Komatsu, T. 2013, *Dalton Trans.*, 42, 15889.
23. Taverna, M., Marie, A.-L., Mira, J.-P. and Guidet, B. 2013, *Ann. Intensive Care*, 3, 4.
24. Roche, M., Rondeau, P., Singh, N. R., Tarnus, E. and Bourdon, E. 2008, *FEBS Lett.*, 582, 1783.
25. Bunn, H. F. and Jandl, J. H. 1968, *J. Biol. Chem.*, 243, 465.
26. Wardell, M., Wang, Z., Ho, J. X., Robert, J., Ruker, F., Ruble, J. and Carter, D. C. 2002, *Biochem. Biophys. Res. Comm.*, 291, 813.
27. Gardner, P. R., Gardner, A. M., Martin, L. A. and Salzman, A. L. 1998, *Proc. Natl. Acad. Sci. USA*, 95, 10378.
28. Gardner, P. R., Gardner, A. M., Brashear, W. T., Suzuki, T., Hvitved, A. N., Setchell, K. D. R. and Olson, J. S. 2006, *J. Inorg. Biochem.*, 100, 542.
29. Eich, R. F., Li, T., Lemon, D. D., Doherty, D. H., Curry, S. R., Aitken, J. F., Mathews, A. J., Johnson, K. A., Smith, R. D., Phillips, G. N. Jr. and Olson, J. S. 1996, *Biochem.*, 35, 6976.
30. Gardner, P. R. 2005, *J. Inorg. Biochem.*, 99, 247.
31. Gardner, A. M. and Gardner, P. R. 2000, *J. Biol. Chem.*, 277, 8166.
32. Gardner, P. R. 2012, *Scientifica*, 2012, 1.
33. Shiva, S., Huang, Z., Grubina, R., Sun, J., Ringwood, L. A., MacArthur, P. H., Xu, X., Murphy, E., Darley-Usmar, V. M. and Gladwin, M. T. 2007, *Circ. Res.*, 100, 654.
34. Galinato, M. G. I., Fogle, R. S. I., Stetz, A. and Galan, J. F. 2016, *J. Inorg. Biochem.*, 154, 7.
35. Brooks, J. 1937, *Proc. Royal Soc. London B. Biol. Sci.*, 123, 368.

36. Sturms, R., DiSpirito, A. A. and Hargrove, M. S. 2011, *Biochem.*, 50, 3873.
37. Huang, K. T., Keszler, A., Patel, N., Patel, R. P., Gladwin, M. T., Kim-Shapiro, D. B. and Hogg, N. 2005, *J. Biol. Chem.*, 280, 31126.
38. Gladwin, M. T. and Kim-Shapiro, D. B. 2008, *Blood*, 112, 2636.
39. Heinecke, J. L., Yi, J., Pereira, J. C. M., Richter-Addo, G. B. and Ford, P. C. 2012, *J. Inorg. Biochem.*, 107, 47.
40. Herold, S. and Rock, G. 2005, *Biochem.*, 44, 6223.
41. Gebicka, L. and Didik, J. 2009, *J. Inorg. Biochem.*, 103, 1375.
42. Sugio, S., Kashima, A., Mochizuki, S., Noda, M. and Kobayashi, K. 1999, *Protein Eng.*, 12, 439.
43. Bhattacharya, A. A., Curry, S. and Franks, N. P. 2000, *J. Biol. Chem.*, 275, 38731.
44. Bhattacharya, A. A., Gruene, T. and Curry, S. 2000, *J. Mol. Biol.*, 303, 721.
45. Zunszain, P. A., Ghuman, J., Komatsu, T., Tsuchida, E. and Curry, S. 2003, *BMC Struct. Biol.*, 3, 6.
46. McWilliam, H., Li, W., Uludag, M., Squizzato, S., Park, Y. M., Buso, N., Cowley, A. P. and Lopez, R. 2013, *Analysis Tool Web Services from the EMBL-EBI. Nucleic Acids Research*.
47. Waterhouse, A. M., Proctor, J. B., Martin, D. M. A., Clamp, M. and Barton, G. J. 2009, *Bioinform.*, 25, 1189.
48. Kamal, J. K. and Behere, D. V. 2002, *J. Biol. Inorg. Chem.*, 7, 273.
49. Hogg, N. and Kalyanaraman, B. 1998, In: M. A. Titheradge (Ed.) *Nitric oxide protocols*. Humana Press Inc. , Totowa, NJ, 231.
50. Storey, K. B. 1996, *Braz. J. Med. Biol. Res.*, 29, 1715.
51. Vazquez-Medina, J. P., Sonanez-Organis, J. G., Burns, J. M., Zenteno-Savin, T. and Ortiz, R. V. 2011, *J. Exp. Biol.*, 214, 2903.
52. Carey, H. V., Frank, C. L. and Seifert, J. P. 2000, *J. Comp. Physiol. B*, 170, 551.
53. Halliwell, B. 1988, *Biochem. Pharmacol.*, 37, 569.
54. Stohs, S. J. and Bagchi, D. 1995, *Free Rad. Biol. Med.*, 18, 321.
55. Gutteridge, J. M. 1986, *Biochim. Biophys. Acta*, 869, 119.
56. Fasano, M., Mattu, M., Coletta, M. and Ascenzi, P. 2002, *J. Inorg. Biochem.*, 91, 487.
57. Roach, M. P., Puspita, W. J. and Watanabe, Y. 2000, *J. Inorg. Biochem.*, 81, 173.
58. Perera, R., Sono, M., Sigman, J. A., Pfister, T. D., Lu, Y. and Dawson, J. H. 2003, *Proc. Natl. Acad. Sci. USA*, 100, 3641.
59. Adachi, S., Shingo, N., Ishimori, K., Watanabe, K. and Morishima, I. 1993, *Biochemistry*, 32, 241.
60. Adachi, S., Nagano, S., Watanabe, H., Ishimori, K. and Morishima, I. 1991, *Biochem. Biophys. Res. Comm.*, 180, 138.
61. Yi, J., Heinecke, J., Tan, H., Ford, P. C. and Richter-Addo, G. B. 2009, *J. Am. Chem. Soc.*, 131, 18119.
62. Wang, B., Shi, Y., Tejero, J., Powell, S. M., Thomas, L. M., Gladwin, M. T., Shiva, S., Zhang, Y. and Richter-Addo, G. B. 2018, *Biochem.*, 57, 4788.
63. Ruetz, M., Kumutima, J., Lewis, B. E., Filipovic, M. R., Lehnert, N., Stemmler, T. L. and Banerjee, R. 2017, *J. Biol. Chem.*, 292, 6512.